Property Investigation of Laser Cladded, Laser Melted and Electron Beam Melted Ti-Al6-V4

Johannes Vlcek
EADS Deutschland GmbH
Corporate Research Centre
P.O. Box 80 04 65
81663 Munich

johannes.vlcek@eads.net

ABSTRACT

Laser or electron beam based powder fusing technologies are interesting processes for structural repair, overhaul of engine components and direct part manufacture. The interesting aspects are low raw material consumption, net shape manufacturing, new dimensional freedom in processing and short lead times to the first part. Currently a variety of processes is being developed mostly by traditional iron based powder melting process developers taking an active part in the development of titanium alloy melting technologies for the medical and aerospace industries. In order to evaluate these technologies for Ti-Al6-V4 structural repair or direct component manufacturing the properties under static and dynamic loading where investigated in this study.

1.0 THE PROCESSES

1.1 Common Process Features

The design freedom in netshape processing results from a direct built up of the parts geometry regardless of considerations if these contours can be machined or not. Consequently complex inner shapes, cooling channels and features alike are possible. As a starting point all powder melting processes use a CAD volume model, which is sliced into layers later being built up one by one. The layer thickness naturally correlates with geometric accuracy and in general ranges from 25-100 µm, but can be considerably lower or higher depending on the process and its objectives. Within each layer the powder melting follows a specific pattern, usually a scan strategy optimised in regard to speed, surface quality and residual stresses generated.

The process technology focused on powder handling, powder melting and feeding of new powder is usually process and manufacturer specific. All processes use argon as a working or cleaning atmosphere rather than nitrogen which will dissolve in titanium as an interstitial alloying element. The main distinctions between the processes can be made in regard to power source and the type of powder handling in a so called powder bed or a welding nozzle.

1.2 Laser Melting in a Powder Bed

The distinct feature of laser melting in a powder bed is the powder bed itself. The process is started on a building plate, melting or welding the first layer of the component (or its support structures) onto the plate. A wiper system will spread a new layer of powder onto the latest layer welded and after each step the building plate is lowered exactly one layer increment. The component is surrounded by loose powder because always the total building space is covered with a new layer of powder. Consequently the final part

Vlcek, J. (2006) Property Investigation of Laser Cladded, Laser Melted and Electron Beam Melted Ti-Al6-V4. In *Cost Effective Manufacture via Net-Shape Processing* (pp. 11-1 – 11-14). Meeting Proceedings RTO-MP-AVT-139, Paper 11. Neuilly-sur-Seine, France: RTO. Available from: http://www.rto.nato.int/abstracts.asp.

has to be removed from loosely stacked powder, the so called powder bed. An opening for hollow geometries is necessary in order to remove residual powder encapsulated.

Generally speaking laser melting in a powder bed offers multiple part manufacture at a time and a good geometric resolution around 0.1 mm. A low heat input during processing can be helpful when specific microstructures need to be avoided. Limitations are the component size - governed by the equipment - only average speed when compared to other types of processes and a need for careful powder handling due to the always present danger of powder contamination. Figure 1 shows the laser in action in the powder bed.

The equipment used in this investigation is a Trumpf Trumaform LF with 130 mm building plate diameter and a 250 W diode pumped disk laser with a variable focus of 200 - 400 µm. The equipment has two building chambers that can be used alternatively and allow a preheating of the building plate up to 500°C to reduce residual stresses. A detailed description of the equipment can be found elsewhere [1].

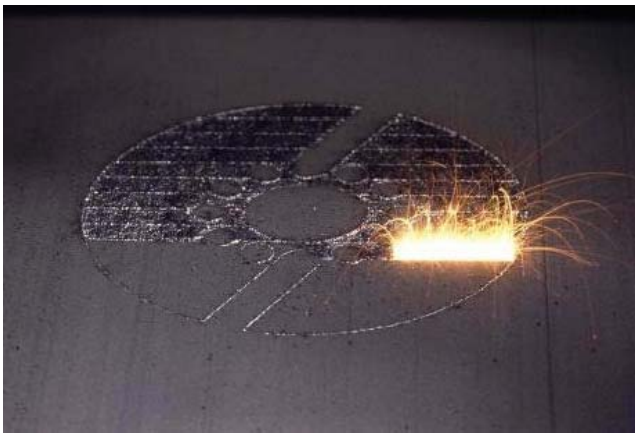

Figure 1: Laser melting in a powder bed [2].

1.3 Electron Beam Melting in a Powder Bed

Electron beam melting has the same principal process features as other powder bed processes. Main differences are the electron beam and the resulting working atmosphere, which naturally is vacuum. The electron beam allows very rapid control of the melting, but a preheating of the powder layer to be welded is required in order to melt the powder particles in place. Nevertheless two of the advantages are an increased speed in material generation and a generally speaking lower content of light element contamination in the Ti-Al6-V4 produced. Size limitations of course exist and the vacuum conditions might lead to a time-temperature profile beneficial to the formation of certain types of microstructure.

In this investigation the ARCAM S12 electron beam melting equipment with a maximum power consumption of 7 kW, scan speed of up to 1000 mm/sec and an accuracy of 400 µm cited by the producer was used. Figure 3 shows parts manufactured by electron beam melting. The weight of the parts can reach about 4.5 kg.

Figure 3: Examples of electron beam melted net shape parts; powder bed [3].

1.4 Laser Cladding

Laser cladding is a technology known for years to reinforce components in specially loaded surface area. Here the term cladding is used for direct metal built up to generate raw shapes and components. The technology uses a coaxial laser head and powder nozzle with the powder being introduced in the melt pool on top of the base plate. Welding bead by welding bead is being deposited side by side. Usually higher deposition rates than in the powder bed are possible, but of course resolution and component detail are limited to the diameter of the laser focus and the accuracy of the translatory unit. Common are mountings on x-y-z gantry units or robots, both enclosed by an inert gas enclosure. New developments consider the use of wire starting material to reduce contamination levels further.

All samples investigated here were produced with a Rofin 3 KW Nd:YAG laser and the IWS coaxial cladding head type COAX8 mounted on a x-y-z translatory unit under argon enclosure. The type of equipment is described in more detail elsewhere [4]. Figure 3 shows the typical process set up without ebclosure.

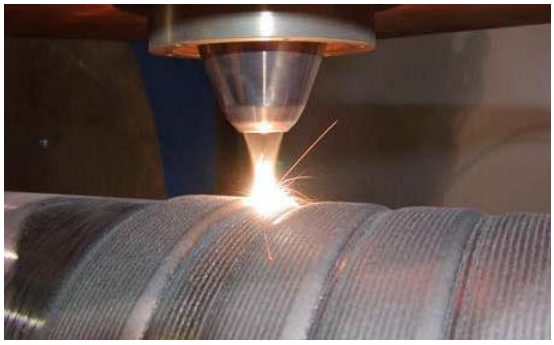

Figure 3: Laser cladding process set up [5].

2.0 MICROSTRUCTURAL FEATURES

2.1 Microstructure

For Ti-Al6-V4 rapid quench microstructures show a needle like structure of α and β phase with prior beta grains. For layered deposition of powders in melting processes such as laser and electron beam melting the beta grains normally grow across the layers deposited following the heat flux in building direction (x-z plane). Length of the β-grains can reach several millimetres in case of cladding processes, with a width

ranging from 200-300µm to up to 1 mm. In a plane perpendicular to the building direction the β-grains look rather globular with a fairly equiaxed structure. Figure 4 shows micrographs of the laser melted, the electron beam melted and the cladded material.

After a heat treatment below β-transus the needle like structure is coarsening dependent on annealing temperature and time changing from needle like martensitic to acicular or Widmanstätten types and eventually to a plate like alpha with beta microstructure. With temperatures above the typical stress relief regime an alpha precipitate is likely to form at the prior β-grain boundaries. Sometimes referred to a structure produced by a quench delay the α-precipitate at β-grain boundaries is typical of non-worked materials being furnace cooled from above the β-transus, a procedure similar to the history of the samples investigated here [6, 7]. Figure 5 shows material samples after annealing at 843°C for 2h and furnace cool as proposed by [8].

Dependent on the temperature-time profile during processing a coarsening of the needle structure is possible during the built up process. The conditions may equal a below β-transus annealing due to the repeated heating of the already deposited Ti-Al6-V4 material. Electron beam melting in vacuum has a higher heat input than laser melting paired with a reduced heat dissipation to the environment due to the vacuum conditions. In detailed analysis of the material a coarser microstructure of Widmanstätten type and about 5-8 µm alpha precipitation can be documented, Figure 6.

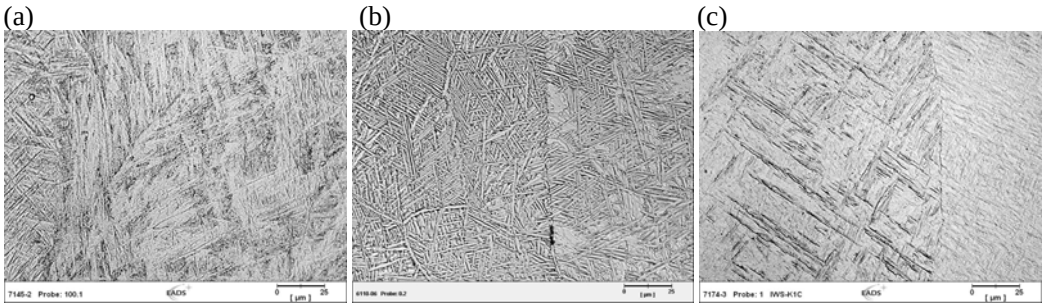

Figure 4: Laser melted (a), electron beam melted (b) and laser cladded (c) Ti-Al6-V4 material. The building direction runs from bottom to top for all micrographs.

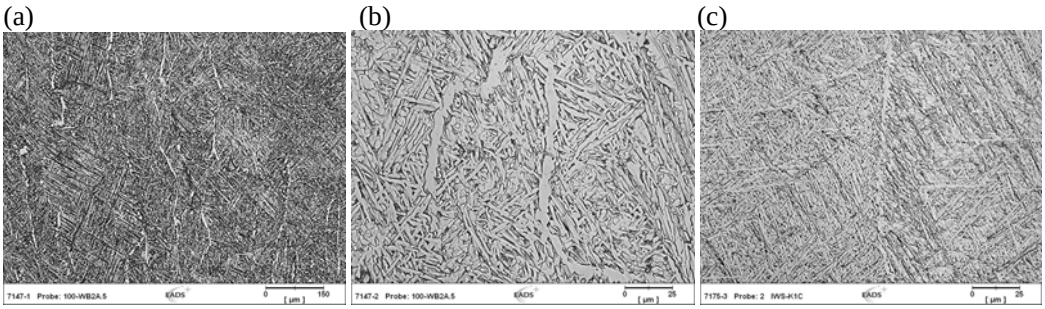

Figure 5: Laser melted (a), (b) and cladded (c) Ti-Al6-V4 after annealing 843°C/2h/furnace cool. The building direction runs from bottom to top for all micrographs.

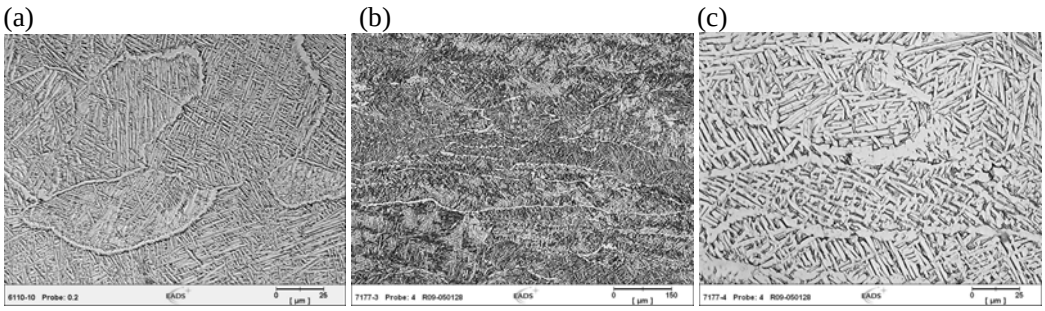

Figure 6: Electron beam melted Ti-Al6-V4 as melted (a) and hot isostatic pressed at 950°C (b) and (c). The building direction runs from left to right for (b) and (c) and is pointing toward the viewer in (a).

2.2 Defects

Typical for all materials generated out of particulate starting material are defects such as gas pores of up to a few microns, elongated pores or missing bond and occasionally not solidified areas which can be detected as pores in a micrograph and show as freely solidified surfaces on a fracture surface. Some materials show fracture (not necessarily brittle) along the built-up layer boundaries. It can not be considered a clear defect, but can be an indication of reduced adhesion, possibly a result of the scanning strategy and its parameters. The fracture phenomena can be avoided by adjusting the parameters.

Figure 7 shows examples of gas pores and a view of a tensile fracture surface displaying non-melted areas and a partially terrace like feature showing failure along the built up layer boundaries.

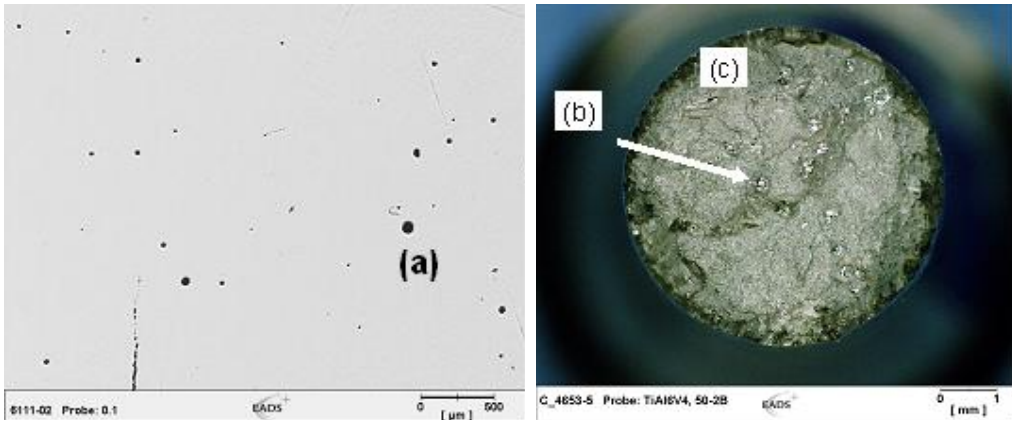

Figure 7: Examples of defects that can be found in laser or electron beam generated Ti-Al6-V4; (a) gas pores, not melted areas (b) and terrace like fracture (c).

2.3 Light Element Contamination

Titanium und titanium alloys are sensitive to light element contamination due to interstitial solution of hydrogen, nitrogen and oxygen. The consequence is anisotropic lattice distortion, changes dislocation movement and glide [9]. Light element contamination therefore leads to a strength increase and loss of ductility until brittle fracture makes the material uninteresting for use. Naturally the working gas

atmosphere can not be air or nitrogen. The laser based processes usually use argon to provide a protective atmosphere. In electron beam melting the working environment is vacuum due to the nature of electron beam physics.

In powder based processes the natural baseline is the contamination of the starting powder. Lower limits can be identified around 1200-1300 ppm depending on powder particle size. Coarser fractions might yield slightly lower levels, but for fractions of 20-100 µm values of 1300-1500 ppm can be considered typical. Over storage time the contamination can slightly increase depending on temperature, humidity and atmosphere. Good experiences were made when storing powders under argon and powder containers in argon filled barrels or glove boxes.

In laser melting processes oxygen pick up is dependent on the quality of the working gas, elimination of possibly degassing materials inside the processing chamber and a gas tight enclosure. Since electron beam melting is performed under vacuum it has a considerable advantage in regard to contamination as long as possible degassing of materials is minimized. Powder contamination values can be kept or under careful processing can even be reduced. Typical oxygen contamination is around 1500 ppm for electron beam melted material and around 1600-1900 ppm or more for other processes. Nitrogen contamination can range from less than 50 ppm to several hundred ppm.

3.0 MECHANICAL PROPERTIES

Static properties of Ti-Al6-V4 produced by generative processes are usually readily available from the process developers. Therefore this activity focused on the acquisition of high cycle fatigue data and fracture toughness. Not all materials were tested in house and for all modes of loading. Valuable high cycle fatigue testing results on electron beam melted material were produced by Fruth Innovative Technologies FIT [10] and Heinl [11]. Arcam AB publishes data sheets on static tensile properties, which account for the data cited here [12]. A more detailed analysis of static properties and evolution after heat treatments was performed on the laser melted material. High Cycle Fatigue and fracture toughness investigation focused on the laser cladded material.

3.1 Static Tensile Testing

Static tensile yield and ultimate strength of generated Ti-Al6-V4 usually can reach around 1000 MPa and almost 1100 MPa respectively. Elongation depends on the process, the degree of melting and possibly on the orientation of the specimen. Table 2 shows either tested or published values. It is apparent that the laser processed materials reach static tensile strength values very much alike. The material melted in the powder bed shows a considerably lower elongation to fracture (5.8%). For the five samples tested a standard deviation of 0.6 was measured. The electron beam melted material shows excellent elongation to fracture values of up to 16% according to the data published. Reduction of area values were communicated to EADS in excess of 40%.

A heat treatment can influence the static tensile properties greatly. Figure 8 shows the effect of different heat treatments on yield strength, ultimate tensile strength, elongation and reduction of area of the laser melted material.

A standard annealing, termed “anneal”, around 700°C shows elongation values below 2%. After a mill annealing at 843°C/2h, labelled “MA”, elongation reaches values around 5%. The elongation could be increased up to 9.7%, standard deviation 2.2, by increasing the duration of the mill annealing treatment, “6 x MA”. Stress relief treatments below 600°C can not improve elongation values; yield strength and ultimate strength are almost identical and the fracture is brittle. The Youngs Modulus decreases less than 5% from 116 to 112 GPa for the two conditions MA and 6 x MA respectively. Micro hardness

measurements on the laser melted material (laser nozzle) lead to a hardness of 376 HV1 (Hardness Vickers) for the as melted condition and 362 HV1 for the anneal state "MA".

Table 2: Static tensile properties of the Ti-Al6-V4 materials in building direction.

Process	Laser melted	Electron beam	Laser cladded
Condition	Mill annealed	As built	As built
Yield Strength [MPa]	1000	910 - 960	1010
Ultimate Strength [MPa]	1083	970 - 1030	1090
Elongation [%]	5.8	12 - 16	12.2
Reduction of Area [%]	9.2	(>>30%)	21
Youngs Modulus [GPa]	116	120	116
Source	*EADS*	*Arcam*	*EADS*

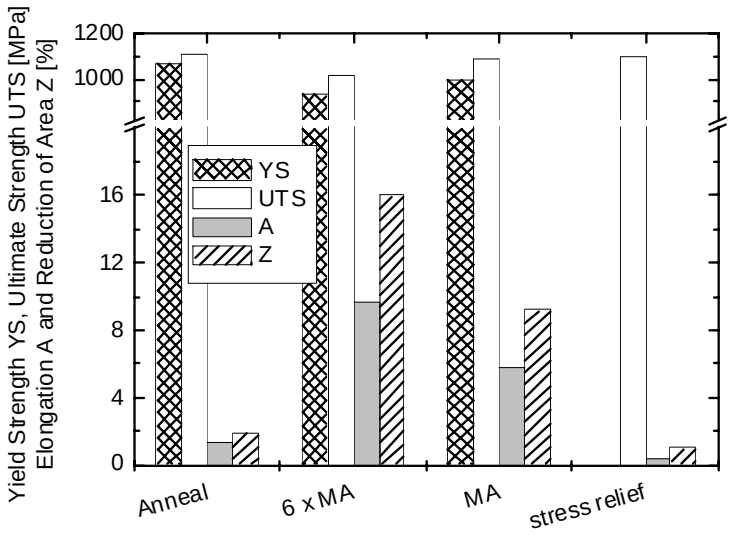

Figure 8: Tensile strength in building direction of laser melted material after specific heat treatments [EADS].

3.2 High Cycle Fatigue Testing

Hour glass shaped specimens with a minimum diameter of 5 mm were machined out of the shapes deposited and tested according to test procedure DIN 50 100 at room temperature. A maximum test frequency 110 Hz with a load ratio of R = 0.1was used. A total of nine samples in the as built condition and five samples in the condition "MA" after 843°C/2h annealing were tested.

A fatigue life of 10^7 cycles can be determined at about 600 MPa for the as built condition, Figure 9. Specific for the test are two groups of failure depending on the stress level: one group well below 10^6

cycles at stress levels between 700 - 750 MPa, the other group around 10^7 cycles loaded with stress levels between 600 - 650 MPa. Specific for the two groups is the site of crack initiation on the sample fracture surface. A rapid failure is observed for samples that have a crack initiation close to or on the surface of the sample located on the outside of the fracture surface. It is assumed that rapid crack initiation (besides a higher stress level) accounts for the early failure. Other than that the fracture surfaces show no unexpected features besides standard dynamic fracture area, residual forced fracture and a few defects.

The heat treatment seems not to improve the situation. For four samples tested at 650 MPa a fatigue life between roughly 7 x 10^5 and 4 x 10^6 cycles was measured. The scatter in fatigue life can be attributed to defects and a rapid crack initiation. Crack initiation at the surface can not be linked to lower cycles clearly. The micro-structural characterization shows a change in the alloys microstructure during the annealing procedure. The α-phase precipitate at the prior grain boundaries is known to have a lower strength in cyclic loading. Additionally the slightly decreasing hardness of about 4% indicates a decrease in yield strength, that would have a similar effect.

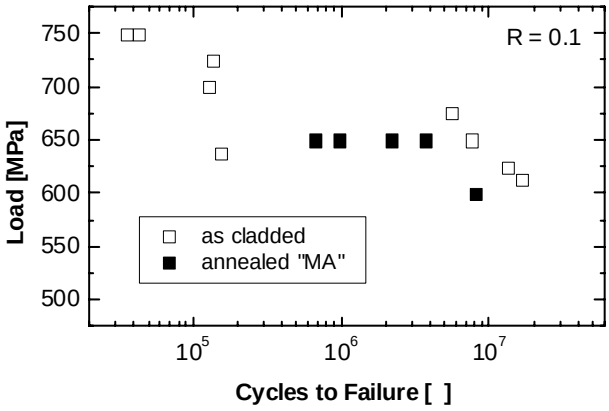

Figure 9: HCF properties in building direction of laser cladded Ti-Al6-V4 tested in the as-built and the annealed state.

Heinl [10] investigated the dependency of fatigue life on sample orientation for electron beam melted Ti-Al6-V4 material, Figure 10.

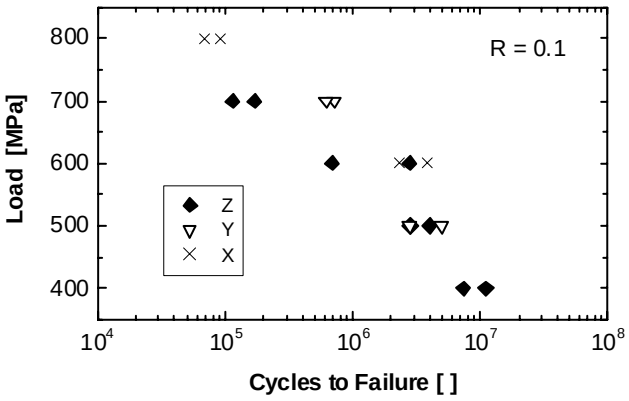

Figure 10: HCF Properties as a function of specimen orientation; EB melted samples [Heinl, 10]

The results show a slightly higher fatigue life for samples with specimen orientation in the building plane x-y as opposed to the building direction z. Defects and reduced bond strength between layers have the largest effect when testing in x-z orientation (the building direction). At lower load levels fatigue life seems to be comparable and there is a similar scatter in the data. The slightly lower values can be explained with the different microstructure – some α-precipitate at the prior grain boundaries with a width of about 2-5 µm, comparable to the microstructure shown in Figure 6 (a) – and a higher number of defects in the electron beam melted samples at this point of development.

3.3 Fracture Toughness Testing

Fracture toughness testing was performed according to ASTM E399-90 on laser cladded material in the T-L and L-T direction determined by the β-grain orientation. Orientation T-L refers to a crack plane parallel to the β-grains (in building direction), orientation L-T refers to crack plane perpendicular to the β-grain orientation (perpendicular to building direction), Figure 11. The as-built and the 843°C/2h mill annealed (MA) condition were tested.

A Fracture toughness of K_{IC} = 63 MPa√m was measured in the as-built condition. The mill annealing procedure "MA" increased fracture toughness to greater than K_Q = 80 MPa√m. Values in β-grain orientation or perpendicular to it only differ slightly regardless of the strong texture in the material. K_{IC} is invalid for the tested specimens with a thickness B of 15 mm in the annealed state because the relation $2.5(Kq/Rp0,2)^2 < B = 15$ mm is not satisfied.

Fracture toughness in [MPa√m]			
as built		mill annealed "MA"	
T-L	L-T	T-L MA	L-T MA
63.2	62.8	84.4	83.8
63.9	60.8	85.3	80.9
K_{IC} valid		K_q	

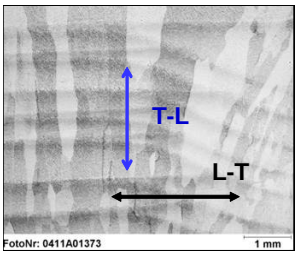

Figure 11: Measured fracture toughness values depending on grain orientation.

Figure 12 shows the fracture surface of the as built fracture toughness specimen after testing. The grain orientation can easily be detected on the T-L fracture surface with the crack path presumably following the β-grain boundaries. In L-T direction another structure is visible that consists of about 3-4 mm wide lines running through the sample. It can be attributed to the weld beads deposited with some overlap side by side in each layer. Both β-grains and weld bead structure are broken up to some extent by the mill anneal treatment showing a fracture surface with slightly "dissolved" features (no picture).

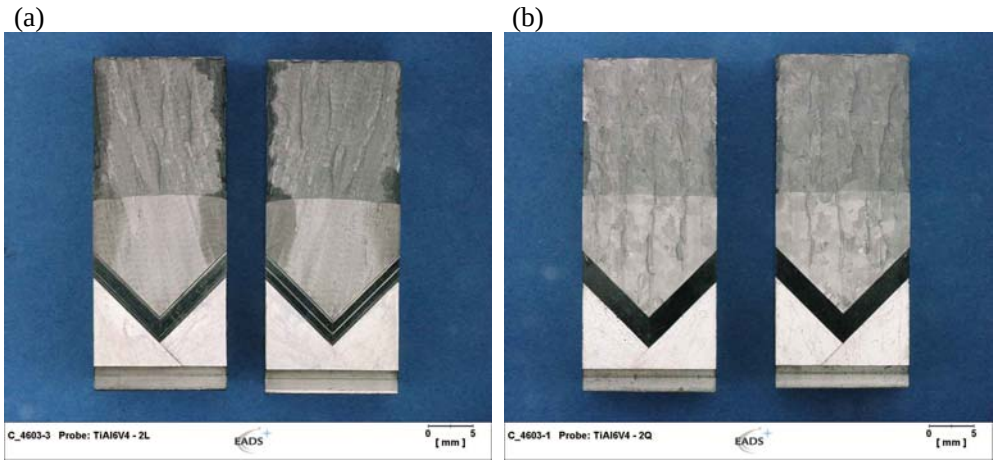

Figure 12: Fracture surface of the laser cladded Ti-Al6-V4 fracture toughness specimen after testing; (a) as-built, T-L direction, (b) as built, L-T direction.

4.0 CONCLUSIONS

In the three investigated processes, laser cladding, laser melting and electron beam melting, powder is melted in layers or welds and rapidly solidifies forming the bulk material. Solidification slightly varies in temperature and time, but comparable microstructure can be documented that differs only little in the morphology of $\alpha-\beta$ precipitation. Defect such as gas pores or non-melted spots can be found in all materials but mainly in the materials produced in the powder bed. Contamination with oxygen can be controlled below 2000 ppm where as electron beam melting delivers materials with oxygen contamination comparable to the feedstock level.

Mechanical Properties of the materials produced is well comparable to cast and even forged material as long as defect size and numbers are kept to low values. Yield strength, ultimate strength and Youngs modulus are comparable between the discussed processes. There is a dependency on dwell time around 800-900°C which leads to slightly lower strength and modulus for electron beam melted material but comes with excellent elongation to fracture up to 16%. In laser cladding Ti-Al6-V4 almost equally high elongation was acquired. One characteristic of the laser cladding approach is the about ¾ overlap of each layer, which leads to very dense material.

For laser melted material a heat treatment is necessary to achieve elongation beyond 5% today. The samples tested in the “weak” building direction showed the bond strength between layers. In processing only a small layer overlap is used in order to reach a more economic deposition speed. Consequently the material elongation is greatly improved in the heat treatment due to inter-layer-diffusion. Elevated heat treating temperature and prolonged time both increase elongation while reducing Youngs modulus and strength slightly.

HCF testing of laser cladded Ti-Al6-V4 shows a considerable scatter in the as built and in the mill annealed “MA” condition. The location of the defect in the sample has a strong influence on crack initiation and cycles to failure. In the mill anneal procedure hardness values decrease slightly and α-precipitate forms at the prior β-grain boundaries, both an indication for lower fatigue life. Fatigue life for 10^7 cycles is around 600 MPa. The directional dependencies found in the electron beam melted material can be explained by the strong impact of defects on the bond strength between layers.

Fracture toughness in the laser cladded Ti-Al6-V4 only varies slightly in and perpendicular to the β-grain structure formed due to the directional built up of the material. The mill anneal heat treatment has a positive influence on fracture toughness. The texture in the material can be documented on the fracture surface of the fracture toughness samples and is slightly broken up by heat treatment. There is a need for defining a more adequate annealing procedure to further improve a balanced fatigue and fracture toughness property profile. In further testing the sample size needs to be adjusted in order to produce valid K_{IC} values.

The net shape processes tested in this investigation deliver interesting properties for Ti-Al6-V4 with each process opening its niche for specific applications. As main differences geometric accuracy, surface quality and deposition rate can be distinguished besides a strong limitation in size for the powder bed based processes. Figure 13 shows a potential candidate component manufacture by laser melting in the powder bed. In a cost analysis cost of powder feedstock, effort for data processing, beam time, post machining or surface treatment have to be accounted for. Even if the cost of components exceed manufacturing cost of common processes by far, a business case might be identified when analysing life cycle cost, cost of design changes and lead times.

Figure 13: Ti-Al6-V4 demonstrator part manufactured by laser melting in the powder bed.

5.0 ACKNOWLEDGEMENTS

A group of people contributed to this study and their effort has to be acknowledged. Sven Orban manufactured the laser cladded shapes at IWS Fraunhofer Dresden. Alexander Bohnke of Fruth Innovative Technologies (FIT), Parsberg, supplied the electron beam melted samples. Peter Heinl at the University of Erlangen performed detailed investigations on the electron beam melted material and shared many of his results in the discussion. Frank-Peter Wüst and Patrick Tröscher of Trumpf, Ditzingen, were very valuable partners in the development of laser beam melting supplying samples and demonstrators. The in-house activities at EADS Corporate research were supported by Karl-Heinz Süss, Elvira Reuder, Christian Plander, Ronald Hauser and Vitus Holzinger in heat treatments, metallography and mechanical testing respectively.

6.0 RFERENCES

[1] Trumpf website and process description, www.trumpf.com

[2] J. Hufless, R. Ganter, M. Lindemann, Trumpf Laserformen – neue generative Laserschweißverfahren für den Werkzeug und Formenbau, Seminar Rapid Manufacturing, IWB Produktionstechnisches Anwenderzentrum Augsburg, Juli 2004

[3] ARCAM EBM S12 description, www.arcam.com.

[4] K.-H. Hermann, S. Orban, S. Nowotny, Laser Cladding of Titanium Alloy Ti6242 to Restore Damaged Blades, Proceedings of the 23rd International Congress on Application of Laser and Electro-Optics 2004

[5] Courtesy of Steffen Nowotny, IWS Dresden.

[6] RMI Titanium Company, Metallography, Brochure on Ti-Al6-V4 and other titanium alloys.

[7] Welsch G., Boyer R., Collings E.W., Materials Properties Handbook: Titanium Alloys, 2. Auflage, ASM International, Materials Park, Ohio, 1998

[8] Charles S.C. Lei, Andrew Davis, Eui W. Lee, Effect of BSTOA and mill anneal on the mechanical properties of TiAl6V4 castings, Advanced Materials and Processes (AMP), ASM International, May 2000, S. 75-77

[9] M. Peters, C. Leyens, Titan und Titanlegierungen,
Wiley VCH, Weinheim 2002

[10] Fruth Innovative Technologien GmbH, Parsberg, Communication, 2005/2006

[11] P. Heinl, Grundlagenuntersuchungen zum Rapid Prototyping von Titan-Bauteilen mittels Elektronenstrahlschmelzen, Thesis, University Erlangen, January 2006

[12] Data sheets on Ti-Al6-V4 and Ti-Al6-V4ELI, www.arcam.com

MEETING DISCUSSION – PAPER NO: 11

Author: J. Vlcek

Discusser: X. Wu

Question: Do you see more porosity in powder bed samples?

Response: Generally there is more porosity in powder bed sample. Still porosity is limited to single pores or sinking defects mostly located at layer interfaces.

Discusser: R. Lang

Question: Why is powder bed laser technology lower in properties in respect to nozzle based processes?

Response: The static properties of both materials are more or less compatible. Elongation is generally a little less with powder bed, fatigue properties are lower. Reason might be sources of contamination in the powder bed, less overlap when melting or open potentials in scan strategy.

Discusser: P. Carroll

Question: For laser clad components, what was O_2 ppm within Ar process chamber?

Response: IWS Dresden used technical pure Ar gas. O-contamination in deposited material could be kept below 2000 ppm.